Nonlinear Dynamics and Systems Theory, **20** (4) (2020) 439–450

Stability of the Artificial Equilibrium Points in the Low-Thrust Restricted Three-Body Problem when the Smaller Primary is an Oblate Spheroid

Md. Sanam Suraj [1], Amit Mittal [2], Krishan Pal [3*] and Deepak Mittal [4]

[1] *Department of Mathematics, Sri Aurbindo College, University of Delhi, New Delhi, India*
[2] *Department of Mathematics, A.R.S.D. College, University of Delhi, New Delhi, India*
[3] *Department of Mathematics, Maharaja Agrasen College, University of Delhi, New Delhi, India*
[4] *Department of Computer Science, Deen Dayal Upadhaya College, University of Delhi, New Delhi-110021, India*

Received: December 27, 2019; Revised: October 2, 2020

Abstract: The aim of this paper is to study the existence and stability of the artificial equilibrium points (AEPs) in the low-thrust restricted three-body problem when the smaller primary is an oblate spheroid and the bigger one is a point mass. The AEPs are obtained by cancelling the gravitational and centrifugal forces with continuous low-thrust at a non-equilibrium point. The AEPs are calculated numerically and their movement is shown graphically. The positions of these AEPs will depend on the magnitude and directions of the low-thrust acceleration. Firstly, we have linearized the equations of motion of the spacecraft. The linear stability of the AEPs is studied. We have drawn the stability regions in the $x-y$, $x-z$ and $y-z$-planes and studied the effect of the oblateness parameter $A \in (0,1)$ on the motion of the spacecraft. Further, we have determined the zero velocity curves to study the possible boundary regions of motion of the spacecraft. Finally, we have concluded about the effects of the relevant parameters in this problem.

Keywords: *restricted three-body problem; artificial equilibrium points; low-thrust; stability; oblate spheroid; zero velocity curves.*

Mathematics Subject Classification (2010): 70F07, 70F10, 70F15.

* Corresponding author: mailto:kpal1987@gmail.com

1 Introduction

The classical restricted three-body problem (R3BP) consists of five libration points, three of them are on the straight line joining the primaries, called collinear libration points, and two of them set up equilateral triangle with the primaries. The collinear libration points $L_{1,2,3}$ are always unstable in the linear sense for any value of the mass parameter μ whereas the triangular points $L_{4,5}$ are stable if $\mu < \mu_c = 0.03852...$, see Szebehely [1]. In recent times, many perturbing forces such as oblateness, radiation forces of the primaries, Coriolis and centrifugal forces etc., have been included in the study of the R3BP. Subbarao and Sharma [2] have investigated the non-collinear libration points in the circular restricted three-body problem (CR3BP) by taking the bigger primary as an oblate spheroid and found that these libration points form nearly equilateral triangle with the primaries. Sharma et al. [3] have studied the existence and stability of libration points in the R3BP by considering both the primaries as triaxial rigid bodies. In their study, they have found five libration points, in which two are triangular and the remaining three are collinear. Prado [4] has worked on the space trajectories in the circular restricted three-body problem. Further, he assumed that the spacecraft moves under the gravitational forces of two massive bodies which are in circular orbits. He also investigated the orbits which can be used to transfer a spacecraft from one body back to the same body or to transfer a spacecraft from one body to the respective Lagrangian points L_4 and L_5. Correa et al. [5] introduced two models of the restricted three-body and four-body problems. They have investigated the transfer orbits from a parking orbit around the Earth to the halo orbit in both the dynamical models. Also, they have compared the total velocity increment to both the models.

If continuous low-thrust is used by a spacecraft to balance the gravitational and centrifugal forces, the new equilibrium points appear. These points are usually referred as the Artificial Equilibrium Points (AEPs). The AEP overcomes the position limitation of the classical equilibrium points as it provides a variety of choices for the design of space missions. Therefore, it has been extensively studied by many authors. These studies include the location, stability and periodic orbits of equilibrium points with different types of propulsions such as solar-sail, solar electric propulsion and other low-thrust propulsion.

Farquhar [6] studied the concept of telecommunication systems using the Lagrange points and investigated ballistic periodic orbits about these points in the Earth-Moon system. Dusek [7] and Broschart [8] have studied the stability of equilibrium points with continuous control acceleration. Morimoto et al. [9] have studied the existence and stability of the AEPs in the low-thrust R3BP and found the stable regions. They have used the discriminant of cubic equation and the Descartes sign rule to study the stability of these AEPs. Baig and McInnes [10] have investigated the artificial three-body equilibria for hybrid low-thrust propulsion. In their study, they have introduced a new concept of creating AEPs in the R3BP when the third body uses a hybrid of solar-sail and electric propulsion. Further, Bombardelli and Pelaez [11] have found the locations of AEPs, stability and minimum control acceleration in the CR3BP. Aliasi et al. [12] have proposed a general mathematical model for different propulsion system such as solar-sail, magnetic and electric sail in the CR3BP to study the existence, geometry and stability of AEPs. Furthermore, Ceccaroni and Biggs [13] have investigated the stability conditions and stable regions for the artificial equilibrium points in the low-thrust circular R4BP. In their study, they have obtained eight natural equilibrium points, four of which

are closed to the smaller body. Among the four equilibrium points close to the smaller body, two are stable and two are unstable. Bu et al. [14] have investigated the positions and dynamical characteristic of the AEPs in a binary asteroid system with continuous low-thrust. Recently, Ranjana and Kumar [15] have studied the existence and stability of the AEPs in the circular restricted problem of 2+2 bodies when the shape of a larger mass is taken to be an oblate spheroid. More recently, Sushil et al. [16] have studied the existence and stability of the equilibrium points in the restricted three-body problem with a Geo-Centric satellite including the Earth's equatorial ellipticity.

In this paper, we have studied the existence and linear stability of the AEPs by considering the smaller primary as an oblate spheroid and the bigger one as a point mass. This paper is organized as follows. In Section 2, we have derived the equations of motion of the spacecraft. In Section 3, we have obtained the locations of AEPs. In Section 4, we have derived the stability conditions and stable regions. In Section 5, we have drawn the zero velocity curves. Finally, in Section 6, we have concluded the results obtained.

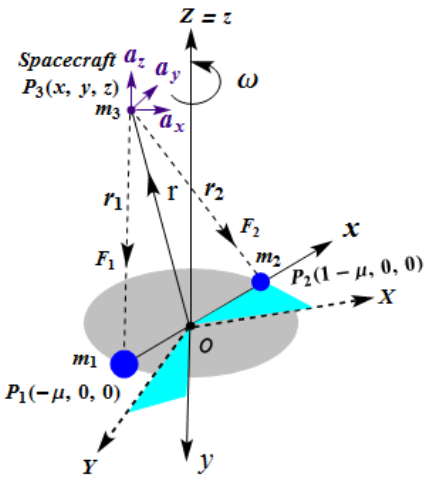

Figure 1: Configuration of the problem.

2 Equations of Motion

Let two celestial bodies of masses m_1 and m_2 $(m_1 > m_2)$ be the primaries moving with angular velocity ω in circular orbits about their center of mass O taken as the origin, and let the infinitesimal body (spacecraft) of mass m_3 be moving in the plane of motion of m_1 and m_2. The motion of the spacecraft is effected by the motion of m_1 and m_2 but not affects them. We shall determine the equations of motion of the infinitesimal body of mass m_3 in dimensionless synodic variables. The line joining the primaries m_1 and m_2 is taken as the X-axis, and the line which passes through the origin O and perpendicular to the OX-axis and is lying in the plane of motion of m_1 and m_2 is considered as the Y-axis, the line which passes through the origin and is perpendicular to the plane of motion of the primaries is taken as the Z-axis. In a synodic frame,

the system of synodic coordinates $O(xyz)$ is initially coincident with the system of inertial coordinates $O(XYZ)$, rotating with the angular velocity ω about the Z-axis (the z axis is coincident with the Z-axis). Let the primaries of masses m_1 and m_2 be located at $P_1(-\mu, 0, 0)$ and $P_2(1-\mu, 0, 0)$, respectively, and the spacecraft be at the point $P_3(x, y, z)$(see Fig. 1). The angular velocity of the primaries is given by the relation $\omega = \sqrt{\frac{G(m_1+m_2)}{l^3}}$, where l is the distance between the primaries, and G is the Gravitational constant. We scale the units by taking the sum of the masses and the distance between the primaries both equal to unity. Therefore, $m_1 = 1-\mu$, $m_2 = \mu$ and $\mu = \frac{m_2}{m_1+m_2}$ with $m_1 + m_2 = 1$. Also, the scale of the time is chosen so that the gravitational constant is unity. The equation of motion of the spacecraft in vector form is expressed as

$$\frac{d^2\mathbf{r}}{dt^2} + 2\boldsymbol{\omega} \times \frac{d\mathbf{r}}{dt} = \boldsymbol{a} - \bigtriangledown\Omega = \mathbf{F}, \tag{1}$$

where Ω is the potential (McCuskey [17]) of the system that combines the gravitational potential and the potential from the centripetal acceleration which is defined as

$$\Omega = -\frac{n^2}{2}(x^2+y^2) - \frac{(1-\mu)}{r_1} - \frac{\mu}{r_2} - \frac{\mu A}{2r_2^3},$$

and

$$\begin{aligned}
\mathbf{F} &= \text{total force acting on} \quad m_3, \\
&= \mathbf{F_1} + \mathbf{F_2}, \\
\mathbf{F_1} &= \text{gravitational force exerted on} \quad m_3 \quad \text{due} \\
&\quad \text{to} \quad m_1 \quad \text{along} \quad \mathbf{P_3P_1}, \\
\mathbf{F_2} &= \text{gravitational force exerted on} \quad m_3 \quad \text{due} \\
&\quad \text{to} \quad m_2 \quad \text{along} \quad \mathbf{P_3P_2}.
\end{aligned}$$

The vector $\boldsymbol{a} = (a_x, a_y, a_z)$ is the low-thrust acceleration and $\mathbf{r} = (x, y, z)^T$ is the position vector of the spacecraft from the origin. Thus, the equations of motion of the spacecraft with continuous low-thrust in the dimensionless co-ordinate system can be written as (Morimoto et al. [9])

$$\left.\begin{aligned}
\ddot{x} - 2\,n\,\dot{y} &= -\Omega_x + a_x = -\Omega_x^*, \\
\ddot{y} + 2\,n\,\dot{x} &= -\Omega_y + a_y = -\Omega_y^*, \\
\ddot{z} &= -\Omega_z + a_z = -\Omega_z^*,
\end{aligned}\right\} \tag{2}$$

where Ω^* is the effective potential of the system with continuous low-thrust and can be written as

$$\Omega^* = \Omega - a_x x - a_y y - a_z z = -\frac{n^2}{2}(x^2+y^2) - \frac{(1-\mu)}{r_1} - \frac{\mu}{r_2} - \frac{\mu A}{2r_2^3} - a_x x - a_y y - a_z z,$$

where $r_1 = \sqrt{(x+\mu)^2 + y^2 + z^2}$, $r_2 = \sqrt{(x+\mu-1)^2 + y^2 + z^2}$, $a = \sqrt{{a_x}^2 + {a_y}^2 + {a_z}^2}$, and n is the mean motion of the primaries which is also defined as $n^2 = (1 + \frac{3A}{2})$, where A is the oblateness parameter of m_2 which is defined as $A = \frac{a_1^2 - c_1^2}{5\,l^2}, 0 < A < 1, a_1 = b_1 (a_1 > c_1)$, where a_1, b_1, c_1 are the semi-axes of the rigid-body of mass m_2, and l is the distance between the primaries.

3 Calculation of the Artificial Equilibrium Points

The AEPs are the solution of the equations $\Omega_x^* = 0$, $\Omega_y^* = 0$, $\Omega_z^* = 0$. The AEPs denoted by (x_0, y_0, z_0) are the solution of the equations given by

$$\left.\begin{aligned} -n^2 x_0 + \frac{1-\mu}{r_1^3}(x_0+\mu) + \frac{\mu}{r_2^3}(x_0-\mu_1-1)\left(1+\frac{3A}{2r_2^2}\right) - a_x = 0, \\ -n^2 y_0 + \frac{1-\mu}{r_1^3} y_0 + \frac{\mu}{r_2^3} y_0 \left(1+\frac{3A}{2r_2^2}\right) - a_y = 0, \\ \frac{1-\mu}{r_1^3} z_0 + \frac{\mu}{r_2^3} z_0 \left(1+\frac{3A}{2r_2^2}\right) - a_z = 0. \end{aligned}\right\} \tag{3}$$

When $A = 0$, $\boldsymbol{a} = (0, 0, 0)$, the above Eqs. (3) reduce to the equations obtained by Szebhely [1]. When $A = 0$, the above Eqs. (3) reduce to the equations obtained by Morimoto et al. [9]. Solve the Eqs. (3) for $z = 0$, then the AEPs are the intersection of $\Omega_x^* = 0$ and $\Omega_y^* = 0$. We have obtained five AEPs for given parameters denoted by L_1, L_2, L_3, L_4 and L_5. The numerical values of the AEPs are shown in Tables 1, 2. From Table 1, we have observed that there exist three collinear and two non-collinear AEPs when low-thrust acceleration is varying in the x direction. From Table 2, we have observed that there exist five non-collinear AEPs for the fixed values of $\mu = 0.1$, $\boldsymbol{a} = (0, 0.0001, 0)$ and for the increasing values of the oblateness parameter A.

We have displayed the movements of AEPs shown graphically in Fig. 2(a, b). In Fig. 2(a), we have plotted the AEPs for the fixed values of $\mu = 0.1$, $A = 0.01$ and for the increasing values of $\boldsymbol{a} = (a_x, 0, 0)$. From Fig. 2 (a), we have observed that when $\boldsymbol{a} = (a_x, 0, 0)$ is increasing, the movements of the AEPs L_1, L_2, and L_3 are almost negligible whereas the AEPs L_4 and L_5 move towards the y-axes. The AEPs L_4 and L_5 are symmetric with respect to the x-axis.

In Fig. 2(b), we have plotted the AEPs for the fixed values of $\mu = 0.1$, $\boldsymbol{a} = (0, 0.0001, 0)$ and for the increasing values of the oblateness parameter A. From Fig. 2 (b), we have observed that when A is increasing, the AEPs L_1 and L_2 move from right to left towards the primaries m_1 and m_2, respectively, whereas the AEP L_3 is shifted from left to right towards the bigger primary m_1 and the AEPs L_4 and L_5 move towards the x-axis. Also, we have noticed that the AEPs L_4 and L_5 are not symmetric with respect to the x-axis. We have observed that the AEPs are the new positions of the equilibrium points, with the effect of continuous low-thrust acceleration and oblateness parameters, which are different from the natural equilibrium points.

$\mu = 0.1$ $A = 0.01$				
$\boldsymbol{a}$	L_1	L_2	L_3	$L_{4,5}$
$(0.0001, 0, 0)$	(0.595693, 0)	(1.27013, 0)	(-1.03681, 0)	(0.394700, $\pm$0.863321)
$(0.01, 0, 0)$	(0.595064, 0)	(1.26863, 0)	(-1.03989, 0)	(0.356034, $\pm$0.880338)
$(0.03, 0, 0)$	(0.593786, 0)	(1.26563, 0)	(-1.04616, 0)	(0.254245, $\pm$0.918441)
$(0.05, 0, 0)$	(0.592501, 0)	(1.26267, 0)	(-1.05252, 0)	(0.0946093, $\pm$0.957963)

Table 1: The AEPs when the low-thrust acceleration $\boldsymbol{a} = (a_x, 0, 0)$ is varying in the x-direction.

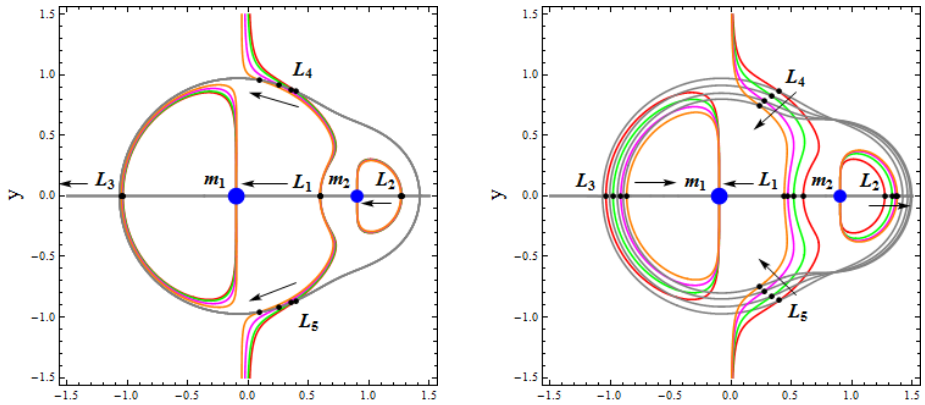

Figure 2: Locations of five AEPs in the low-thrust R3BP for $\mu = 0.1$ under the effect of low-thrust acceleration and oblateness parameters $\boldsymbol{a}$, A, respectively, (a) for $A = 0.01$ and for different values of $\boldsymbol{a} = (0.0001, 0, 0)\,(gray, red)$, $(0.01, 0, 0)\,(gray, green)$, $(0.03, 0, 0)\,(gray, magenta)$, $(0.05, 0, 0)\,(gray, orange)$, and (b) for $\boldsymbol{a} = (0, 0.0001, 0)$ and for different values of $A = 0.01\,(gray, red)$, $0.15\,(gray, green)$, $0.35\,(gray, magenta)$, $0.55\,(gray, orange)$

$\mu = 0.1$ $\boldsymbol{a} = (0, 0.0001, 0)$		
A	L_1	L_2
$A = 0.01$	(0.595700, 0.0000172961)	(1.27015, 0.0000656752)
$A = 0.15$	(0.517147, 0.0000140423)	(1.33094, 0.0000541839)
$A = 0.35$	(0.469174, 0.0000122795)	(1.35954, 0.0000424306)
$A = 0.55$	(0.438985, 0.0000112294)	(1.37323, 0.0000347701)
L_3	L_4	L_5
(-1.036780, 0.001068400)	(0.395227, 0.863036)	(0.394896, -0.863275)
(-0.977898, 0.000824811)	(0.336840, 0.826193)	(0.336620, -0.826353)
(-0.913935, 0.000611650)	(0.277461, 0.782479)	(0.277319, -0.782585)
(-0.864974, 0.000479622)	(0.234858, 0.746633)	(0.234756, -0.746711)

Table 2: The AEPs in the $x - y$-plane when the oblateness parameter A is varying.

4 Stability Analysis and Stable Region

For establishing the spacecraft at a non-equilibrium point, a continuous low-thrust is provided to the spacecraft. Now, we give the small displacement to (x_0, y_0, z_0) as $x = x_0 + \delta_x$, $y = y_0 + \delta_y$, $z = z_0 + \delta_z$, $(\delta_x, \delta_y, \delta_z << 1)$. Using the above displacements, the linearized equations corresponding to Eqs. (2) according to Morimoto et al. [9] are given

by

$$\left.\begin{aligned} \ddot{\delta_x} - 2n\dot{\delta_y} &= (\Omega^*_{xx})^0\delta_x + (\Omega^*_{xy})^0\delta_y + (\Omega^*_{xz})^0\delta_z, \\ \ddot{\delta_y} + 2n\dot{\delta_x} &= (\Omega^*_{yx})^0\delta_x + (\Omega^*_{yy})^0\delta_y + (\Omega^*_{yz})^0\delta_z, \\ \ddot{\delta_z} &= (\Omega^*_{zx})^0\delta_x + (\Omega^*_{zy})^0\delta_y + (\Omega^*_{zz})^0\delta_z, \end{aligned}\right\} \tag{4}$$

where the superscript '0' in Eqs. (4) indicates that the values are to be calculated at the AEP (x_0, y_0, z_0). Further, the characteristic root λ satisfies

$$\left.\begin{aligned} &\lambda^6 + ((\Omega^*_{xx})^0 + (\Omega^*_{yy})^0 + (\Omega^*_{zz})^0 + 4\,n^2)\,\lambda^4 + ((\Omega^*_{xx})^0(\Omega^*_{yy})^0 \\ &+(\Omega^*_{xx})^0(\Omega^*_{zz})^0 + (\Omega^*_{yy})^0(\Omega^*_{zz})^0 - ((\Omega^*_{xy})^0)^2 - ((\Omega^*_{xz})^0)^2 - ((\Omega^*_{yz})^0)^2 \\ &+4\,n^2\,(\Omega^*_{zz})^0)\,\lambda^2 + (\Omega^*_{xx})^0(\Omega^*_{yy})^0(\Omega^*_{zz})^0 + 2\,(\Omega^*_{xy})^0(\Omega^*_{xz})^0(\Omega^*_{yz})^0 \\ &-((\Omega^*_{xy})^0)^2(\Omega^*_{zz})^0 - ((\Omega^*_{xz})^0)^2(\Omega^*_{yy})^0 - ((\Omega^*_{yz})^0)^2(\Omega^*_{xx})^0 = 0. \end{aligned}\right\} \tag{5}$$

Taking $k = \lambda^2$, we have obtained

$$\left.\begin{aligned} &k^3 + ((\Omega^*_{xx})^0 + (\Omega^*_{yy})^0 + (\Omega^*_{zz})^0 + 4\,n^2)\,k^2 + ((\Omega^*_{xx})^0(\Omega^*_{yy})^0 \\ &+(\Omega^*_{xx})^0(\Omega^*_{zz})^0 + (\Omega^*_{yy})^0(\Omega^*_{zz})^0 - ((\Omega^*_{xy})^0)^2 - ((\Omega^*_{xz})^0)^2 - ((\Omega^*_{yz})^0)^2 \\ &+4\,n^2\,(\Omega^*_{zz})^0)\,k + (\Omega^*_{xx})^0(\Omega^*_{yy})^0(\Omega^*_{zz})^0 + 2\,(\Omega^*_{xy})^0(\Omega^*_{xz})^0(\Omega^*_{yz})^0 \\ &-((\Omega^*_{xy})^0)^2(\Omega^*_{zz})^0 - ((\Omega^*_{xz})^0)^2(\Omega^*_{yy})^0 - ((\Omega^*_{yz})^0)^2(\Omega^*_{xx})^0 = 0. \end{aligned}\right\} \tag{6}$$

We see that the Eqn. (6) is a cubic equation in k and it can be written as

$$k^3 + d_1k^2 + d_2k + d_3 = 0, \tag{7}$$

where

$$\begin{aligned} d_1 &= (\Omega^*_{xx})^0 + (\Omega^*_{yy})^0 + (\Omega^*_{zz})^0 + 4\,n^2, \\ d_2 &= (\Omega^*_{xx})^0(\Omega^*_{yy})^0 + (\Omega^*_{xx})^0(\Omega^*_{zz})^0 + (\Omega^*_{yy})^0(\Omega^*_{zz})^0 - ((\Omega^*_{xy})^0)^2 \\ &\quad -((\Omega^*_{xz})^0)^2 - ((\Omega^*_{yz})^0)^2 + 4\,n^2\,(\Omega^*_{zz})^0, \\ d_3 &= (\Omega^*_{xx})^0(\Omega^*_{yy})^0(\Omega^*_{zz})^0 + 2\,(\Omega^*_{xy})^0(\Omega^*_{xz})^0(\Omega^*_{yz})^0 - ((\Omega^*_{xy})^0)^2(\Omega^*_{zz})^0 \\ &\quad -((\Omega^*_{xz})^0)^2(\Omega^*_{yy})^0 - ((\Omega^*_{yz})^0)^2(\Omega^*_{xx})^0. \end{aligned}$$

Here, we shall study the linear stability of the AEPs by calculating the characteristic roots of Eqn. (7). As we know that, all the characteristic roots of a cubic equation are either real numbers or one of them is a real number and the other characteristic roots are imaginary numbers. A necessary and sufficient condition for an AEP to be linearly stable is that all the characteristic roots of Eqn. (5) lie in the left-hand side of the λ-plane (i.e., $\lambda \leq 0$). If one or more characteristic roots of Eqn. (5) lie in the right-hand side of the λ-plane, then the AEP is always unstable. If all the characteristic roots of Eqn. (5) lie to the left-hand side of the λ-plane, then Eqn. (7) must have three real and negative roots. The resulting linear stability conditions according to Morimoto et al. [9] and Descartes sign rule are $D \geq 0$, $d_1 > 0$, $d_2 > 0$ and $d_3 > 0$, where D is the

discriminant of the cubic Eqn. (7) and is given by

$$D = \frac{1}{4}\left(d_3 + \frac{2\,d_1^3 - 9\,d_1\,d_2}{27}\right)^2 + \frac{1}{27}\left(d_2 - \frac{d_1^2}{3}\right)^3. \tag{8}$$

Eventually, we have concluded that the system of AEPs is linearly stable when $D \geq 0$, $d_1 > 0$, $d_2 > 0$ and $d_3 > 0$.

Furthermore, we have plotted the stability regions in the $x-y$, $x-z$ and $y-z$-planes as shown in Fig. 3(a, b, c, d, e, f). From Fig. 3, we have observed that the stability regions reduce around both the primaries for the increasing values of the oblateness parameter $A \in (0, 1)$. According to stability theory, it is concluded that the AEPs located in the stable regions are linearly stable, otherwise unstable. Further, it is concluded that the stable AEPs in these stable regions can be obtained by designing the magnitude and direction of the low-thrust acceleration for space missions.

5 Zero Velocity Curves

The Jacobi integral of the equations of motion is defined as

$$C = 2\Omega + (\dot{x}^2 + \dot{y}^2 + \dot{z}^2). \tag{9}$$

The Jacobi integral of the equations of motion with continuous low-thrust is defined as

$$C' = 2\Omega^* + (\dot{x}^2 + \dot{y}^2 + \dot{z}^2). \tag{10}$$

We have drawn the ZVCs from Eq. (10) by taking $\dot{x} = \dot{y} = \dot{z} = 0$. The white domains correspond to the Hill region, and the cyan color indicates the forbidden regions, while the thick black lines show the ZVCs. In these ZVCs, the black dots indicate the positions of the AEPs, while the blue dots indicate the positions of two primaries m_1 and m_2. In Fig. 4, we have drawn the ZVCs for $\mu = 0.1$, $A = 0.01$, $\boldsymbol{a} = (0,\, 0.0001,\, 0)$ and for the different values of the Jacobi constant C'. The ZVCs in Fig.4(a, b, c, d) are labeled as $C' = -3.640439$, $C' = -3.415439$, $C' = -3.116439$ and $C' = -2.945439$, respectively.

Fig. 4 (a) indicates the ZVC for the value of the Jacobi constant $C' = -3.640439$ and shows that, there exists a circular land (white domains) around both the primaries and the spacecraft trapped in these regions, where the motion is possible and the circular strip (the cyan color) shows the forbidden region where the motion is not possible. Thus, the spacecraft can move around both the primaries and can not move from one primary to other. Fig. 4 (b) shows the ZVC for $C' = -3.415439$, it is observed that the spacecraft can freely move in the entire white domain. In Fig. 4 (c), there exist a limiting situation for $C' = -3.116439$ and a cusp at L_3, it is observed that the spacecraft can freely move in the entire white domain. In Fig. 4 (d), the curves of zero velocity constitute two branches for $C' = -2.945439$. The first branch contains L_4 and the other branch contains L_5. Also, the curves split into two parts at L_3 and shrink to the tadpole shaped curves around L_4 and L_5. Hence, there is only forbidden region around L_4 and L_5 in the tadpole shaped region and the spacecraft is free to move everywhere in the plane. We have observed that for the increasing values of the Jacobi constant C', the representing possible boundary regions increase in which the spacecraft can freely move from one place to other place.

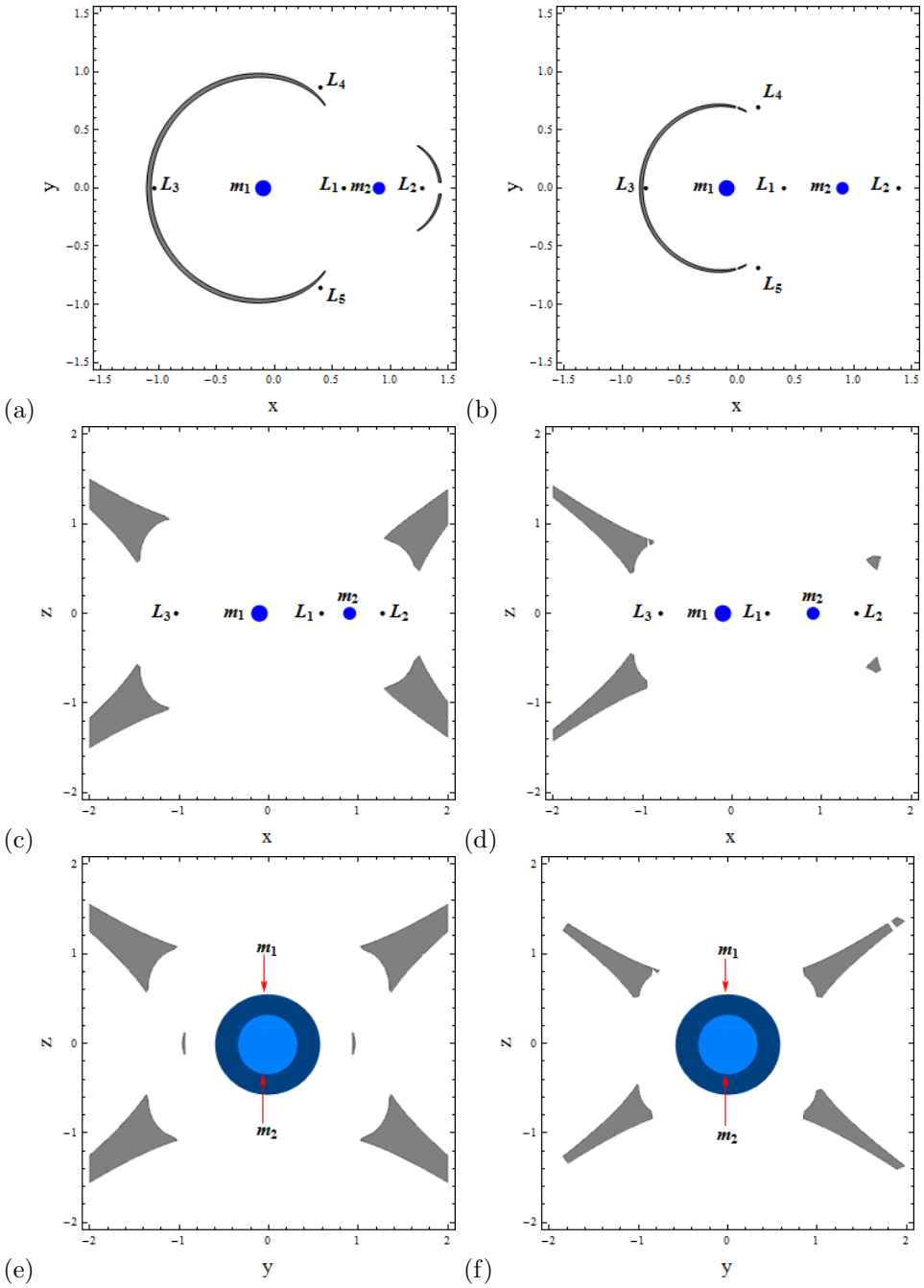

Figure 3: The stable regions (gray area) in the low-thrust R3BP with the effect of oblateness for the mass parameter $\mu = 0.1$, panels-(a, b) in the $x - y$-plane for $A = 0.01,\ 0.95$, respectively, panels-(c, d) in the $x - z$-plane for $A = 0.01,\ 0.95$, respectively, and panels-(e, f) in the $y - z$-plane for $A = 0.01,\ 0.95$, respectively.

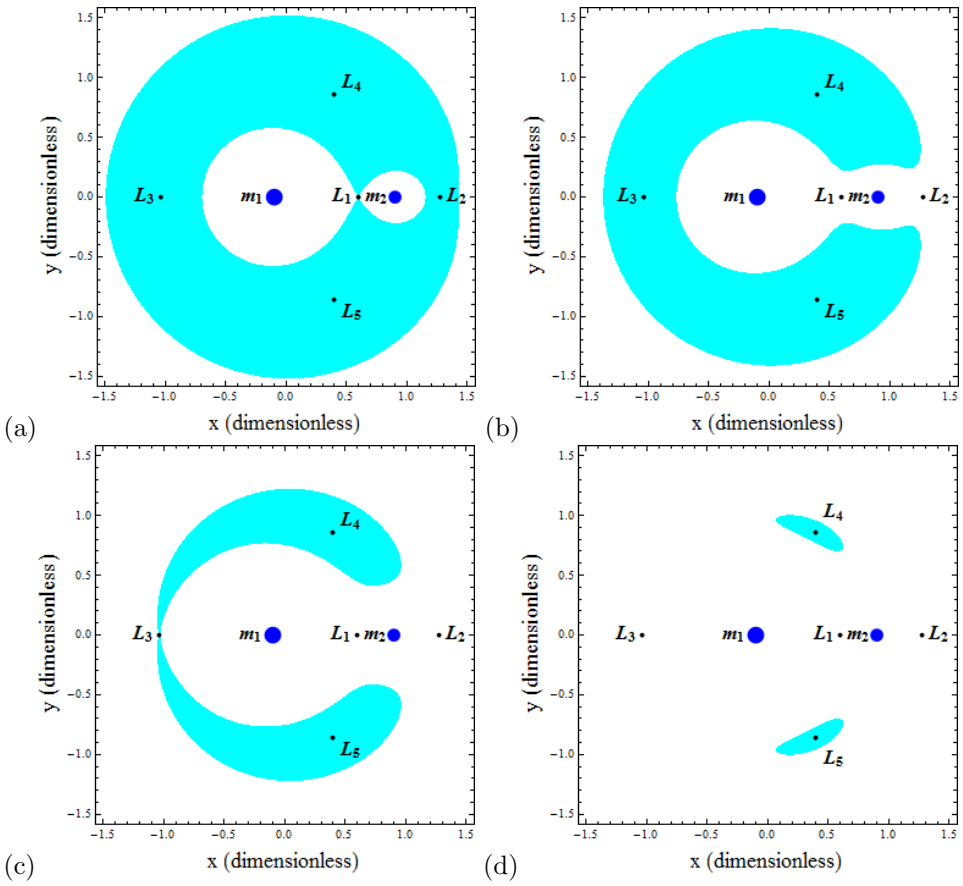

Figure 4: Zero velocity curves for the fixed values of $\mu = 0.1$, $A = 0.01$, $\boldsymbol{a} = (0, 0.0001, 0)$ and for the different values of the Jacobi constant C', (a) for $C' = -3.640439$, (b) for $C' = -3.415439$, (c) for $C' = -3.116439$ and (d) for $C' = -2.945439$.

6 Conclusion

In this paper, we have studied the existence and stability of the AEPs in the low-thrust R3BP problem when the smaller primary is an oblate spheroid and the bigger one is a point mass. The AEPs are obtained by introducing the continuous control acceleration at the non-equilibrium points. The numerical values of the AEPs are shown in Tables 1, 2. We have observed that there exist three collinear and two non-collinear AEPs at the low-thrust acceleration varying in the x direction whereas there exist only five non-collinear AEPs at the low-thrust acceleration in the y direction. The movements of AEPs are shown graphically in Fig. 2. We have observed that the non-collinear points L_4 and L_5 are symmetrical about the x-axis at the low-thrust acceleration varying in the x direction. We have derived the equations of motion of the spacecraft in the synodic coordinate system. Further, we have transformed these equations of motion into a six-degree equation. Also, the six-degree equation has been transformed into a cubic equation and we found the conditions for analyzing linear stability. The effect of the oblateness parameter $A \in (0, 1)$ is studied on the motion of the spacecraft. We have plotted the stability regions in the $x-y$, $x-z$ and $y-z$-planes as shown in Fig. 3. From Fig. 3, we have observed that the stability regions reduce near both the primaries m_1 and m_2 for the increasing values of the oblateness parameter $A \in (0, 1)$.

Our results are different from those by Morimoto et al. [9] in some aspects, namely, (i) they have obtained the AEPs in the low-thrust R3BP, whereas we have obtained the AEPs in the low-thrust R3BP with the effect of the oblateness of the smaller primary. In our case, the AEPs are new positions of natural equilibrium points different from those by Morimoto et al. [9] due to the presence of the oblateness parameter $A\,(0 < A < 1)$. When the oblateness parameter $A = 0$, then the results obtained in this work are in agreement with those by Morimoto et al. [9]. When $\boldsymbol{a} = (0,\, 0,\, 0)$ and $A = 0$, the obtained results are in agreement with the results by Szebehely [1]; (ii) they have found the stability regions in the Sun-Earth system, whereas we have found the stability regions for $\mu = 0.1$ and for different values of the oblateness parameter $A\,(0 < A < 1)$. Finally, we have drawn the ZVCs to determine the possible regions of motion of the spacecraft in which the spacecraft is free to move. We have observed that for the increasing values of the Jacobi constant C', the possible regions of motion increase, in which the spacecraft can freely move from one place to another. This paper is applicable in the Sun-Earth system for communications of the spacecraft missions.

Acknowledgment

We are very thankful to the **Centre of Fundamental Research in Space Dynamics and Celestial Mechanics (CFRSC)**, New Delhi, India for giving some necessary study materials and other supporting things which are required for the present research work.

References

[1] V. Szebehely. *Theory of Orbits, the Restricted Problem of Three-Bodies*. Academic press, New York, 1967.

[2] P. V. Subbarao and R. K. Sharma. A note on the stability of the triangular of equilibrium points in the restricted three-body problem. *Astron. Astrophys.* **43** (1975) 381–383.

[3] R. K. Sharma, Z .A. Taqvi and K. B. Bhatnagar. Existence of libration points in the restricted three-body problem when both the primaries are triaxial rigid bodies. *Indian J. Pure Appl. Math.* **32**(1) (2001) 125–141.

[4] A. F. B. A. Prado. A survey on space trajectories in the model of three-bodies. *Nonlinear Dynamics and Systems Theory* **6** (4) (2006) 389–400.

[5] A. A. Corrêa, A. Prado, T. J. Stuchi and C. Beaugé. Comparison of transfer orbits in the restricted three and four-body problems. *Nonlinear Dynamics and Systems Theory* **7** (3) (2007) 267–277.

[6] R. W. Farquhar. Lunar communications with libration point satellites. *Spacecraft and Rockets.* **4**(10) (1967) 1383–1384.

[7] H. M. Dusek. Motion in the vicinity of libration points of a generalized restricted three-body model. *Prog. Astronaut. Rocket.* **17** (1966) 37–54.

[8] S. B. Broschart and D. J. Sheeres. Control of hovering spacecraft near small bodies: Application to Asteroid 25143 Itokwa. *J. Guid. Control Dyn.* **28**(2) (2005) 343–354.

[9] M. Y. Morimoto, H. Yamakawa and K. Uesugi. Artificial equilibrium points in the low-thrust restricted three-body problem. *J. Guid. Control Dyn.* **30**(5) (2007) 1563–1567.

[10] S. Baig and C. R. McInnes. Artificial three-body equilibria for hybrid low-thrust propulsion. *J. Guid. Control Dyn.* **31** (6) (2008) 1644–1655.

[11] C. Bombardelli and J. Pelaez. On the stability of artificial equilibrium points in the circular restricted three-body problem. *Celest. Mech. Dyn. Astron.* **109**(1) (2011) 13–26. Doi.10.1007/s10569-010-9317.

[12] G. Aliasi, G. Mengali and A. Quarta. Artificial equilibrium points for a generalized sail in the circular restricted three-body problem. *Celest. Mech. Dyn. Astron.* **110** (2011) 343–368.

[13] M. Ceccaroni and J. Biggs. Extension of low-thrust propulsion to the autonomous coplanar circular restricted four-body problem with an application to future Trojan asteroid missions. *Celest. Mech. Dyn. Astron.* **112** (2012) 191–219.

[14] Shichao Bu, Shuang Li and Hongwei Yang. Artificial equilibrium points in binary asteroid systems with continuous low-thrust. *Astrophys. Space Sci.* **362** (137) (2017). Doi.10.1007/s10509-017-31197-7.

[15] K. Ranjana and V. Kumar. On the artificial equilibrium points in the circular restricted problem of 2+2 bodies. *Int. J. Astron. Astrophys.* **7**(4) (2017) 239–249.

[16] S. Yadav, V. Kumar and R. Aggarwal. Existence and stability of equilibrium points in the restricted three-body problem with a Geo-Centric satellite including the Earth's equatorial ellipticity. *Nonlinear Dynamics and Systems Theory* **19** (4) (2019) 537–550.

[17] S. W. McCusky. *Introduction to Celestial Mechanics.* Addision-wesley publishing company. Inc. New York, 1963.